Thermophysical study of 2-acetylthiophene: experimental and modelled results

V. Antón, H. Artigas, J. Muñoz-Embid, M. Artal, C. Lafuente*

Departamento de Química Física, Facultad de Ciencias, Universidad de Zaragoza, 50009 Zaragoza, Spain.

*Corresponding author. Tel: +34 976762295, E-mail address: celadi@unizar.es

Abstract

Several thermophysical properties have been studied for 2-acetylthiophene: (i) vapour pressure was determined at temperatures within 336.16 - 445.02 K; (ii) density, speed of sound, static permittivity, refractive index, surface tension, and kinematic viscosity were measured at $\boldsymbol{p}$ = 0.1 MPa and at temperatures from 278.15 K (or 283.15 K for the refractive index) to 338.15 K; (iii) volumetric properties were also determined at temperatures in the (283.15 - 338.15) K range and at pressures up to 65.0 MPa. From these experimental values, different derivative properties have been calculated such as enthalpy of vaporization, isobaric expansibility, isothermal and isentropic compressibility, dipole moment, entropy and enthalpy of surface formation, and dynamic viscosity. All experimental properties were correlated and the results were explained through the intermolecular interactions. Moreover PC-SAFT EoS was used to model the thermodynamic behaviour of the compound. Finally, this EoS combined with the Density Gradient Theory allowed obtaining the influence parameter for the surface tension of 2-acetylthiophene.

Keywords: 2-acetylthiophene; thermophysical properties; PC-SAFT.

1. Introduction

Thiophene is a five heterocycle compound with an atom of sulphur and can be extracted, as well as its derivatives, from fossil fuels [1,2]. The presence of thiophene-based compounds in plants provides specific organoleptic characteristics. Thus, it was detected 2-acetylthiophene in different foods such as flour extrudes or yeast extracts producing a sulfurous odor like disinfectant [3,4].

This compound can be employed for various purposes such as: synthesis of several drugs for depressive disorder and anxiety (duloxetine and others) [5,6]; drugs synthesis for treatment of anti-inflammatory [7]; synthesis of antiparasital drugs [8]; metal complexes synthesis [9]; organic synthesis [10]. Despite the many industrial applications of 2-acetylthiophene, the study of its thermophysical properties is very scarce [11,12]. The knowledge of these properties in a wide range of temperature and pressure and its dependence on structure and intermolecular interactions is fundamental in the chemical industry: the volumetric properties give the necessary information about the structural organization and packing of the molecules in liquid state. Furthermore additional information about the intermolecular interactions can be obtained through boiling point, viscosity or surface tension; and the permittivity and refractive index allow to characterize the compound polarity [13-15].

In this contribution, we present experimental values for several properties: (i) vapour pressure from $\boldsymbol{T}$ = 336.16 to 445.02 K; (ii) density in the following pressure and temperature ranges ($\boldsymbol{p}$ = 0.1 to 65 MPa) and ($\boldsymbol{T}$ = 278.15 to 338.15 K); and (iii) speed of sound, static permittivity, surface tension, and kinematic viscosity at $\boldsymbol{p}$ = 0.1 MPa and the temperature interval 278.15 to 338.15 K (or 283.15 to 338.15 K for the refractive index). From these properties, we calculate others such as: enthalpy of vaporization, isobaric expansibility, isothermal compressibility, isentropic compressibility, dipole moment, entropy and enthalpy

of surface formation per unit surface area, and dynamic viscosity. Finallly, we use the PC-SAFT EoS [16] to model the phase, volumetric and acoustic behaviour of the studied compound as well as to find the influence parameter [17] for surface tension.

2. Experimental section

2.1. Chemicals

2-Acetylthiophene was provided by Sigma-Aldrich and the purity was checked by GC chromatography; this purity, expressed as mass percentage, was 99.6 %. An automatic titrator Crison KF 1S-2B was employed to determine the water content of the liquid, being this content less than 100 ppm. Table 1 reports at $\boldsymbol{p}$ = 0.1 MPa the density, ρ, and the refractive index, $\boldsymbol{n}_D$, at $\boldsymbol{T}$ = 293.15 K, and the surface tension, σ, and the dynamic viscosity, η, at $\boldsymbol{T}$ = 303.15 K obtained in this work along with the literature values [11].

Table 1. Density, ρ, refractive index, $\boldsymbol{n}_D$, surface tension, σ, and dynamic viscosity, η, at $\boldsymbol{p}$ = 0.1 MPa and at two temperatures of 2-acetylthiophene. Comparison between experimental and literature values

$\boldsymbol{T}$ = 293.15 K			$\boldsymbol{T}$ = 303.15 K		
Property	Exp.	Lit.	Property	Exp.	Lit.
ρ / (kg·m^{-3})	1171.07	1170.9 [11]	σ / (mN·m^{-1})	42.59	44.5 [11]
$\boldsymbol{n}_D$	1.5658	1.5667 [11]	η / (mPa·s)	2.3157	2.32 [11]

[a]Standard uncertainties $\boldsymbol{u}$ are $\boldsymbol{u}(\boldsymbol{T})$ = 0.005 K for density and $\boldsymbol{u}(\boldsymbol{T})$ = 0.01 K for the rest of properties, $\boldsymbol{u}(\boldsymbol{p})$ = 0.5 kPa, and the combined expanded uncertainties $\boldsymbol{U}_c$ are $\boldsymbol{U}_c(\rho)$ = 0.1 kg· m^{-3}, $\boldsymbol{U}_c(\boldsymbol{n}_D)$ = 10^{-4}, $\boldsymbol{U}_c(\sigma)$ = 1%, $\boldsymbol{U}_c(\eta)$ = 1% with 0.95 level of confidence ($\boldsymbol{k}$ =2).

2.1. Apparatus

Different facilities were used to measure the properties studied in this study, all the devices were periodically checked and rearranged if necessary. An all-glass dynamic recirculating ebulliometer (Fischer-Labodest) equipped with a Cottrell pump allowed determining the vapour pressure, $\boldsymbol{p}_v$, with uncertainties in the temperature and pressure of equilibrium of 0.01 K and 0.05 kPa, respectively. The pressure was measured with a Digiquartz 735-215A-102 pressure transducer (Paroscientific) and the temperature with a thermometer model F25 with a PT100 probe (Automatic Systems Laboratories). The proper operation of the ebulliometer was checked by measuring the vapour pressures of some fluids (hexane, octane and decane).

Density, ρ, and speed of sound, $\boldsymbol{u}$, at atmospheric pressure were simultaneously obtained using an Anton Paar DSA 5000 vibrating tube densimeter and sound analyser (at a frequency of 3 MHz), automatically thermostated at ± 0.005 K. The estimated uncertainties in the measure of density and speed of sound were 0.1 $kg \cdot m^{-3}$ and 0.5 $m \cdot s^{-1}$, respectively. Densities at high pressure were measured by means a high pressure, high temperature Anton Paar DMA HP cell connected to an Anton Paar DMA 5000 unit. The high pressure cell includes a Peltier thermostat to control the temperature, on the other hand to achieve working pressure a hand pump 750.1100 from Sitec (Switzerland) was used, this pressure was measured by a pressure transducer US181 from Measuring Specialties (USA). The uncertainties in this apparatus were: 0.05 MPa in pressure, 0.01 K in temperature and 0.2 $kg \cdot m^{-3}$ in density. The device was calibrated using several fluids (dry air, hexane, water and dichloromethane) of known density, more details about calibration and procedure can be found in our previous paper [18].

A capacitive method was used to determine the static permittivity, ε, at a frequency of 2 MHz. To do this, an Agilent 4263BA precision LCR meter connected to an Agilent 16452A

terminal dielectric test was used. The temperature was controlled by means of a CT52 Schott-Geräte thermostat. The uncertainties for temperature and static permittivity were 0.01 K and 1 %, respectively.

A Digital Abbe Refractometer Zuzi WAY-1S with an external Lauda E-200 thermostat that keeps the temperature constant were used to measure the refractive index at sodium D wavelength (589.3 nm), n_D, being the uncertainty in temperature 0.01 K and the uncertainty in refractive index 10^{-4}.

Surface tension, σ, measurement was carried out by the drop volume technique with a tensiometer Lauda TVT-2. The temperature was controlled by an external Lauda E-200 thermostat. The estimated uncertainties for the temperature and the surface tension were 0.01 K and 1 %, respectively.

Kinematic viscosity, ν, was measured with an Ubbelohde capilar viscosimeter including a Schott-Geräte AVS-440 automatic unit and a CT52 Schott-Geräte thermostat to attain a constant temperature. The uncertainty in temperature is 0.01 K and the uncertainty of kinematic viscosity, expressed as percentage, was 1 %.

3. Model

3.1. PC-SAFT

PC-SAFT EoS is widely described in the literature so that, in this section, we summarize its most important features; all expressions can be found in the paper of Gross and Sadowski [16]. In this model, the dimensionless Helmholtz energy, $\tilde{a}$, is written as a sum of an ideal gas contribution, $\tilde{a}^{id}$, and a residual contribution, $\tilde{a}^{res}$, which is calculated by perturbation theory. The hard-chain fluid is established as a reference system for the repulsive interactions and the attractive ones are considered a disturbance to that. Thus,

$$\tilde{a}^{res} = \tilde{a}^{hc} + \tilde{a}^{dis} + \tilde{a}^{assoc} + \tilde{a}^{polar} \quad (1)$$

where $\tilde{a}^{hc}$ represent the hard-chain contribution obtained from Chapman's approach [19]; $\tilde{a}^{dis}$ is the dispersive attractive contribution calculated using the Barker and Henderson's theory [20,21]; $\tilde{a}^{assoc}$ is the association contribution; and $\tilde{a}^{polar}$ include multipole contributions. In this work, we do not consider multipole interactions and the studied compound is not associated.

It is clear that an advantage of this model is that only three parameters are necessary in order to describe each non-associating pure compound: the chain segment number, m, the segment diameter, σ_{SAFT}, and the segment energy, ε_{SAFT}. Usually, they are obtained by fitting the thermodynamic properties of the compound.

3.2. Density gradient theory

In this theory, extended by Cahn and Hilliard [22], the Helmholtz free energy density for a two-phase system is written as a Taylor series whose expression keeping the two lowest-order terms is:

$$f[\rho(z)] = f_0[\rho(z)] + k_{ii}(T)[\nabla\rho(z)]^2 \quad (2)$$

where $\rho(z)$ is the density of molecules at position z; $f_0[\rho(z)]$ is the free energy in the homogeneous part of the system; and $k_{ii}(T)$ is the influence parameter.

The Helmholtz free energy is calculated as the following:

$$A[\rho(z)] = \int \{ f_0[\rho(z)] + k_{ii}(T)[\nabla\rho(z)]^2 \} dz \quad (3)$$

For a system in equilibrium, this equation has a minimum and this is used to calculate the density profile in the interface. However, it is more adequate to replace the unbounded domain; for this, the z-origin is located at a density $\rho(z_0) = (\rho^v + \rho^l)/2$ being ρ^v and ρ^l

the equilibrium densities for vapor and liquid phases, respectively. The density profile, $\rho(z)$, in the direction perpendicular to the surface can be calculated by:

$$z = z_0 + \int_{\rho^v}^{\rho^l} \sqrt{\frac{k_{ii}(T)}{f_0[\rho(z)] - \rho(z)\mu + p}}\, dz = z_0 + \int_{\rho^v}^{\rho^l} \sqrt{\frac{k_{ii}(T)}{\Delta f[\rho(z)]}}\, dz \qquad (4)$$

where μ is the chemical potential and p is the pressure, for the phases.

Thus, the surface tension can be calculated [22]:

$$\sigma = 2\int_{\rho^v}^{\rho^l} \sqrt{\Delta f[\rho(z)] k_{ii}(T)}\, d\rho(z) \qquad (5)$$

4. Results and discussion

In this section, we have described and discussed the experimental data obtained using the apparatus reported in Section 2 as well as the calculated values for several derived properties. In order to understand the effect of the presence of the acetyl group on the thermophysical properties, we compared the data of this work with those previously published by us for thiophene [23]. Finally, we have modelled the phase and volumetric properties with the PC-SAFT Equation of State and we found the influence parameter for the surface tension.

4.1. Experimental and derived properties

Experimental values for all properties measured in this study (vapour pressure, density at atmospheric pressure (p = 0.1 MPa), density at high pressure, speed of sound, refractive index, static permittivity, surface tension, kinematic viscosity, and dynamic viscosity) along with derived properties (isentropic compressibility, enthalpy of surface formation per unit surface area, and dipole moment) are given in Tables S1-S3 of the Supporting Information.

We have determined the vapour pressure, p_v, of 2-acetylthiophene in the following temperature intervals: T = (336.16 – 445.02) K. The values (Table S1 and Figure 1) were correlated with the Antoine equation:

$$\log p_v = A - \frac{B}{C + t} \tag{6}$$

where p_v is the vapour pressure in kPa, t is the temperature in Celsius degrees, and A, B and C are the adjustable parameters. These fitting parameters and the mean relative deviation, MRD, calculated from the equation 7 and expressed in percentage are presented in Table 2.

$$MRD = \frac{100}{n} \cdot \sum_{i=1}^{n} \left| \frac{Y_{i,cal} - Y_{i,exp}}{Y_{i,exp}} \right| \tag{7}$$

where n is the data number, and $Y_{i,exp}$ and $Y_{i,cal}$ are the experimental and the calculated values, respectively.

Table 2. Fitting parameters and mean relative deviations, MRD, for the studied properties

Property	*Equation*	*A*	*B*	*C*	*MRD* / %
p_v / kPa	6	6.296	1757.597	195.131	0.59
u / (m·s^{-1})	13	-3.43424	2493.24		0.02
ε	13	-0.14603	32.99		0.32
n_D	13	$-4.758 \cdot 10^{-4}$	1.5722		0.00
σ / (mN·m^{-1})	13	-0.11441	46.01		0.04
η / (mPa·s)	15	0.0903	494.679	150.779	0.13

We have only found a vapour-liquid equilibrium data in the literature [11]. In order to carry out the comparison with our data, we have calculated the boiling point at atmospheric pressure. The obtained value, T_b = 487.68 K, was very close to that determined by Johnson [11] (T_b = 487.05 K). Moreover, Roux et al. [12] studied the thermochemistry of this compound. Our molar enthalpy of vaporization data at T = 298.15 K calculated from the

Clausius-Clapeyron equation, $\Delta \boldsymbol{H}_{vap}$ = 56.03 kJ·mol^{-1}, was lower than the value determined by them using a Calvet microcalorimeter, $\Delta \boldsymbol{H}_{vap}$ = 58.8 kJ·mol^{-1}.

It is known that the vapour pressure decreases with the increasing intermolecular forces and therefore with increasing dipole moment of the compound. Thus, the $\boldsymbol{p}_v$ data measured in this work were lower than those previously determined by us for the thiophene and its derivatives [23].

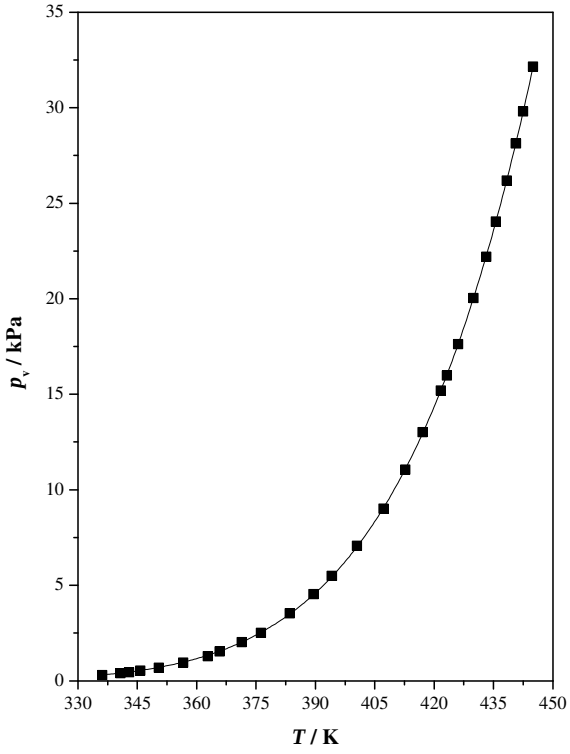

Figure 1. Vapour pressure, $\boldsymbol{p}_v$, of 2-acetylthiophene as a function of temperature.

Regarding the volumetric behaviour, the temperature and pressure ranges studied in this work were: $\boldsymbol{T}$ = (278.15 – 338.15) K and $\boldsymbol{p}$ = (0.1 – 65) MPa. The experimental densities, ρ, (Tables S2 and S3) have been correlated with pressure, $\boldsymbol{p}$, and temperature, $\boldsymbol{T}$, using the TRIDEN model [24]. This equation combines the Tait equation with a modified Rackett equation as Spencer and Danner suggested [25-27].

$$\rho_0 = \frac{A_R}{B_R \left[1+(1-T/C_R)^{D_R}\right]} \tag{8}$$

$$\rho = \frac{\rho_0}{1 - C_T \ln\left(\frac{B_T + p}{B_T + p_0}\right)} \tag{9}$$

$$B_T = b_0 + b_1\left(\frac{T}{E_T}\right) + b_2\left(\frac{T}{E_T}\right)^2 + b_3\left(\frac{T}{E_T}\right)^3 \tag{10}$$

where ρ_0 is the density at p = 0.1 MPa. The fitting parameters together with the mean relative deviation, ***MRD***, are given in Table 3.

Table 3. Parameters of the TRIDEN model and mean relative deviation, ***MRD***

A_R / (kg·m^{-3})	499.240
B_R	0.58546
C_R / K	587.2407
D_R	0.75668
C_T	0.06338
b_o / MPa	361.2466
b_1 / MPa	-67.34008
b_2 / MPa	-33.80525
b_3 / MPa	8.30235
E_T / K	123.35924
MRD / %	0.0073

Figure 2 shows the density values of 2-acetylthiophene as well as the dependence of the density with temperature and pressure described by the derivative properties isobaric expansibility, α_p (± 0.012 kK^{-1}), and the isothermal compressibility, κ_T (± 33 TPa^{-1}), respectively:

$$\alpha_p = \frac{1}{V}\left(\frac{\partial V}{\partial T}\right)_p = -\frac{1}{\rho}\left(\frac{\partial \rho}{\partial T}\right)_p \tag{11}$$

$$\kappa_T = -\frac{1}{V}\left(\frac{\partial V}{\partial p}\right)_T = \frac{1}{\rho}\left(\frac{\partial \rho}{\partial p}\right)_T \tag{12}$$

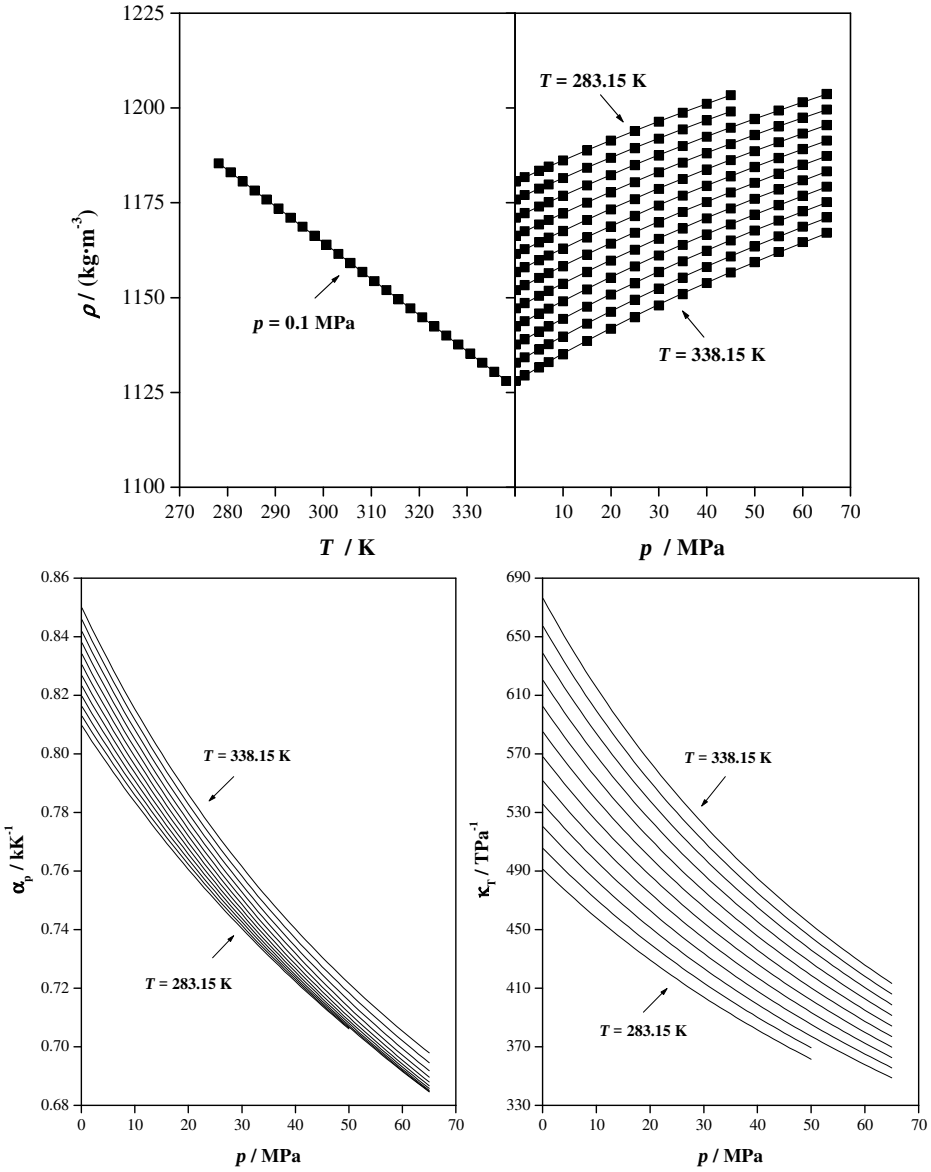

Figure 2. Density, ρ, isobaric expansibility, α_p, and isothermal compressibility, κ_T, of 2-acetylthiophene as a function of temperature and pressure: (■), experimental densities; (—), values calculated with the TRIDEN equation.

The density values decreased with increasing temperature at constant pressure due mainly to thermal expansion. On the other hand, at a given temperature, ρ increased with

pressure. Our data at T = 293.15 K and at atmospheric pressure is in good agreement with the bibliographic value (Table 1). In the same working conditions, density of thiophene (ρ = 1064.530 kg·m^{-3}) was quite smaller than density of 2-acetylthiophene, so the latter compound has better packing. The calculated isobaric expansibilities and isothermal compressibilities can be found in Tables S4 and S5. The α_p values for 2-acetylthiophene are lower than for thiophene due to the presence of stronger molecular interaction. The isothermal compressibility, κ_T, is able to explain the behaviour about structural organization. The small values for this property, κ_T = 535.61 TPa^{-1} at T = 298.15 K and at p = 0.1 MPa, are indicative of a good packing of the 2-acetylthiophene molecules under these conditions.

For the following properties: speed of sound, refractive index, surface tension and static permittivity a linear relationship has been found with respect to temperature, therefore we have employed a linear equation to fit the data with temperature:

$$Y = AT + B \quad (13)$$

where Y is the studied property and A and B are the adjustable parameters. The best fitting parameters along with the corresponding mean relative deviation, ***MRD***, are collected in Table 2.

The variation of the speed of sound, u, for this compound with temperature showed the expected behaviour: the values decreased when the values for temperature increased (Table S2, Figure 3). In fact, we have found a linear relationship: $u = A \cdot T + B$, the parameters A and B and the mean relative deviation, ***MRD***, are listed in Table 2. Comparing the u values for 2-acetylthiophene and thiophene, we have observed that the value for the first compound was higher than the second [23]. Using the experimental values of density and speed of sound at atmospheric pressure, we have obtained the isentropic compressibility, κ_S, from the Newton-Laplace equation, assuming that ultrasonic absorption is negligible ($\kappa_S = 1/(\rho u^2)$). The calculated values at the temperatures studied are listed in Table S2 and are shown in Figure 4.

The study of isentropic compressibility provides important information about internal organization of the molecules: a lower value indicates a more closely packed structure. For 2-acetylthiophene and thiophene at T = 298.15 K, κ_S = 397.42 TPa^{-1} and 578.45 TPa^{-1}, respectively. Again, it is observed the same tendency as previous properties.

We have found again a linear dependence descendant with the temperature for static permittivity, refractive index, and surface tension (Figures 5-7), the corresponding adjustable parameters A and B and the mean relative deviation, MRD, are also collected in Table 2.

Results for static permittivity, ε, (Table S2) show that 2-acetylthiophene exhibits very high values compared with thiophene [23]. For the refractive index, n_D, a better molecular packing leads to higher refractive index values. As seen from compressibility values, the n_D value for 2-acetylthiophene should be larger than for thiophene. On average, at the studied temperatures, the values were approximately 2.5 % higher (Table S2). Our data at T = 293.15 K (Table 1) as well as the variation of refractive index with the temperature be agreed with the literature. We found $(\partial n_D/\partial T)$ = - 4.8·10^{-4} K^{-1} and the data published by Johnson [11] was $(\partial n_D/\partial T)$ = - 4.9·10^{-4} K^{-1}.

In addition, we have obtained the dipole moment of 2-acetylthiophene in the liquid state from our experimental data of density, refractive index and static permittivity, using the Onsager equation [28]:

$$\mu^2 = \frac{9\kappa TM}{4\pi N_A \rho} \frac{\left(\varepsilon - n_D^2\right)\left(2\varepsilon + n_D^2\right)}{\varepsilon\left(n_D^2 + 2\right)^2} \qquad (14)$$

in this equation M, N_A, and k are the molar mass, the Avogadro constant, and the Boltzmann constant, respectively. The calculated dipole moment slightly decreases with temperature. The dipole moment, μ = 3.87 D at T = 298.15 K, is much greater than that found by us [23] for the thiophene. This high value of the dipole moment is due to the combined presence of the carbonyl group and the thiophene ring [29].

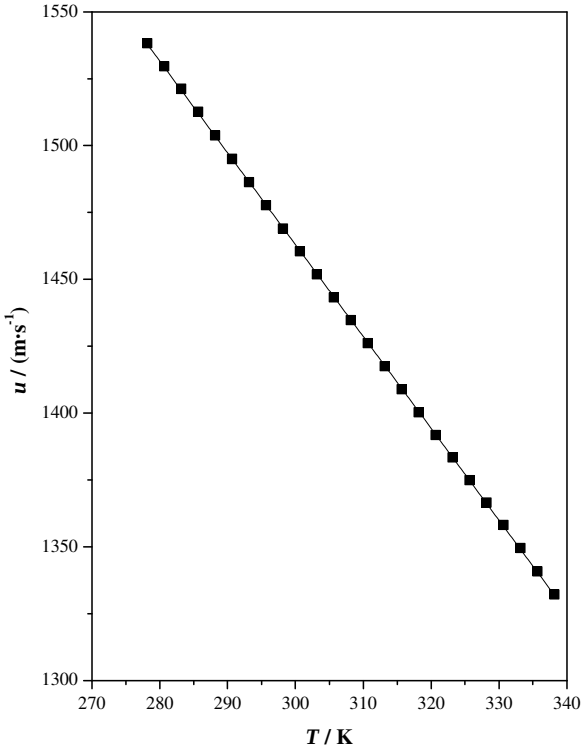

Figure 3. Speed of sound, ***u***, of 2-acetylthiophene at ***p*** = 0.1 MPa as a function of temperature.

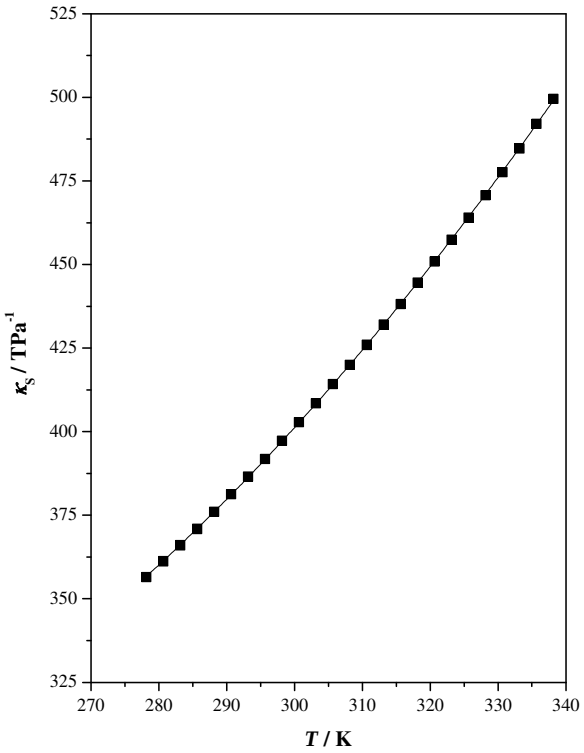

Figure 4. Isentropic compressibility, κ_S, of 2-acetylthiophene at ***p*** = 0.1 MPa as a function of temperature.

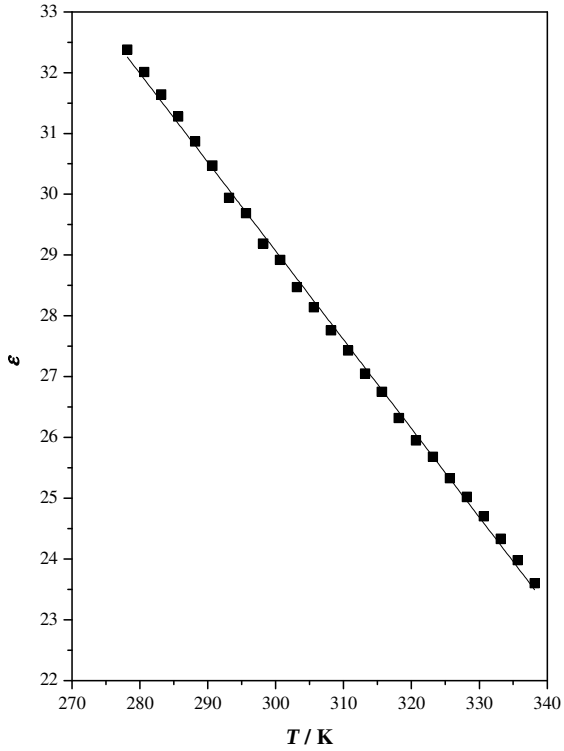

Figure 5. Static permitivity, ε, of 2-acetylthiophene at $\boldsymbol{p}$ = 0.1 MPa as a function of temperature.

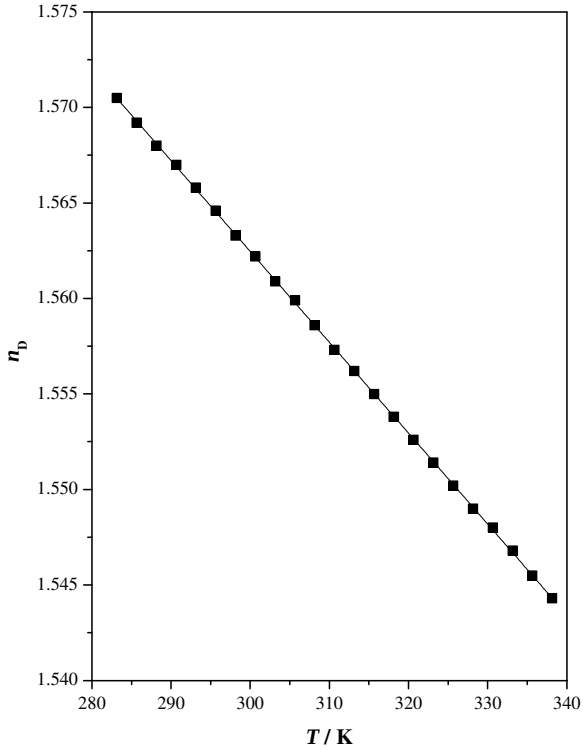

Figure 6. Refractive index, $\boldsymbol{n}_D$, of 2-acetylthiophene at $\boldsymbol{p}$ = 0.1 MPa as a function of temperature.

Surface tension, σ, presents the degree of cohesive forces between liquid molecules. In the bulk of liquids, the forces are equal in all directions because the liquid molecules are surrounded by similar ones. In the surface of liquid/gas interface, the molecules are not surrounded by other molecules in all directions, so the resulting force is attractive into the liquid. The surface tension causes that the molecules in the liquid/gas interface tend to contract in a minimum surface area [30]. It is observed that the surface tension decreased when the temperature increased (Table S2, Figure 7), because the cohesive forces weaken. At $\boldsymbol{T}$ = 303.15 K, our σ value is not agreed with the published by Johnson in 1947 [11] showing a deviation of 1.91 mN.m^{-1}. The result obtained for 2-acetylthiophene was higher than the result obtained for thiophene previously [23] because the interactions between molecules for 2-acetylthiophene were stronger. We have calculated derived properties of surface tension such as the entropy of surface formation per unit surface area, $\Delta \boldsymbol{S}_{\sigma} = -(\partial\sigma / \partial \boldsymbol{T})_{\boldsymbol{p}}$, and enthalpy of surface formation per unit surface area, $\Delta \boldsymbol{H}_{\sigma} = \sigma - \boldsymbol{T}\cdot(\partial\sigma / \partial \boldsymbol{T})_{\boldsymbol{p}}$. As mentioned above, it was found a linear relationship between surface tension and temperature; so the entropy of surface formation per unit surface area was constant in all of range of measurements. On the other hand, it can be also outlined that the enthalpy of surface formation per unit surface area is almost constant over our temperature range. The obtained values for both properties were $\Delta \boldsymbol{S}_{\sigma}$ = 0.1144 mN·m^{-1}·K^{-1} and $\Delta \boldsymbol{H}_{\sigma}$ = 77.27 mN·m^{-1} at $\boldsymbol{T}$ = 298.15 K. The entropy was slightly lower than that found for the thiophene indicating that 2-acetylthiophene is a more structured liquid [23]. On the other hand, the enthalpy was approximately 5 % higher [23], which is related with upper intermolecular interaction energy.

The dynamic viscosity, η, was estimated with an uncertainty of 1 % from our density and kinematic viscosity experimental values: $\eta = \rho \cdot \nu$. These values (Table S2) decreased exponentially with temperature (Figure 8) and they were correlated using a Vogel-Fulcher-Tamman equation [31-33]:

$$\eta = \eta_0 \cdot \exp[\boldsymbol{B}/(\boldsymbol{T} - \boldsymbol{T}_0)] \quad (15)$$

in the above equation, η_0 **,** $\boldsymbol{B}$ and $\boldsymbol{T}_0$ are the adjustable parameters, and they are listed in Table 2 as ***A***, ***B*** and ***C***, respectively. There is a good agreement between the value found in the literature and the experimentally determined here at $\boldsymbol{T}$ = 303.15 K (Table 1). As the 2-acetylthiophene has some strong intermolecular forces, the experimental data show some higher values for this property than the ring of thiophene. We thought that interactions established between the π-electrons for carbonyl group and the π-electrons for thiophene ring [34] were responsible for these results.

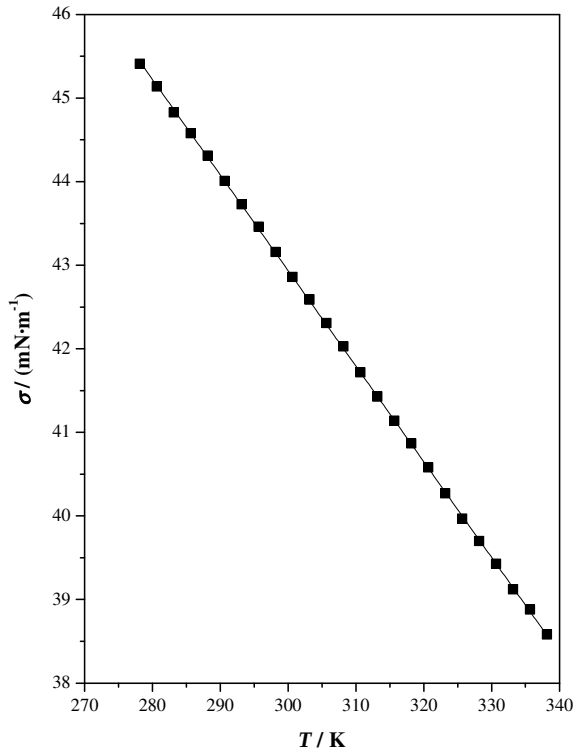

Figure 7. Surface tension, σ, of 2-acetylthiophene at $\boldsymbol{p}$ = 0.1 MPa as a function of temperature.

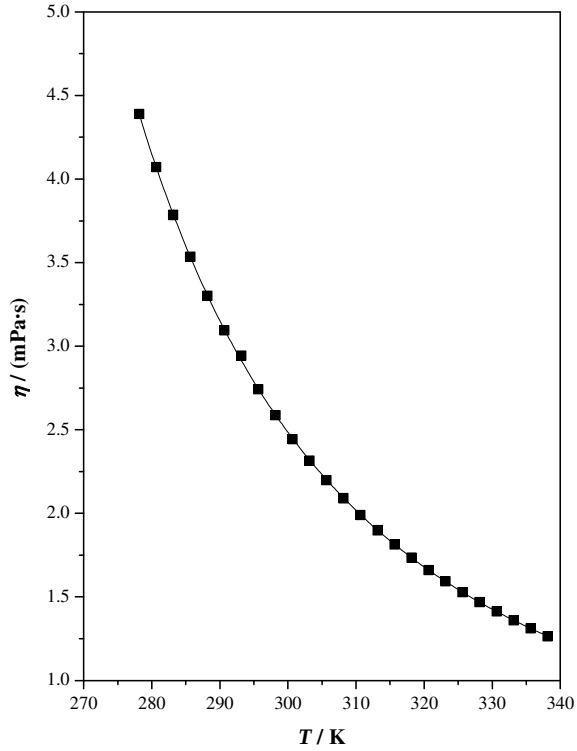

Figure 8. Dynamic viscosity, η, of 2-acetylthiophene at $\boldsymbol{p}$ = 0.1 MPa as a function of temperature.

4.2. Modelling

Our experimental vapour pressures and ***pVT*** data have been used to model the 2-acetylthiophene with PC-SAFT EoS [16]. Table 4 lists the parameters obtained in the modelling of the studied compound by fitting of the above mentioned data. The temperature and pressure working ranges are also included in this Table.

The vapour pressures calculated by the model are in good agreement with the experimental ones. Figure 9 shows the deviations in the comparison between experimental and calculated $\boldsymbol{p}_{\mathrm{v}}$ data. The mean relative deviation (equation 7) was ***MRD*** = 2.33 %. Due to the small vapour pressure values, we also calculated the deviation as average absolute deviation, $\boldsymbol{AAD}_{\mathrm{p}}$, between experimental and calculated vapour pressures:

$$AAD_p = \frac{1}{n}\sum_{i=1}^{n}\left|p_{i,cal} - p_{i,exp}\right| \quad (16)$$

it can be outlined that the value obtained, AAD_p = 0.11 kPa, is only twice the experimental uncertainty.

Table 4. 2-Acetylthiophene PC-SAFT parameters: m, σ_{SAFT}, and ε_{SAFT} together with temperature-dependent influence parameter, $k_{ii} = f(T)$, and temperature and pressure working ranges

M / (g·mol^{-1})	126.176
m	4.0086
σ_{SAFT} / Å	3.3626
(ε_{SAFT}/k) / K	303.84
k_{ii} / 10^{-19} J·m^5·mol^{-2}	$2.45 + 4.97\cdot10^{-3}T$
T_{range} / K	278.15 - 445.02
p_{range} / MPa	$3\cdot10^{-4}$ - 65

For the density, PC-SAFT EoS underestimated the values at atmospheric pressure in almost all the working temperature range and the deviation increased with increasing temperature (Figure 10). The mean relative deviation at the working temperature range was: MRD = 0.21 %. Moreover, the values obtained using PC-SAFT EoS for the density of compressed liquid, ρ, are in good agreement with the experimental ones and both intersect at intermediate pressures (Figure 10). The relative deviations obtained range from -0.38 to +0.62 % with a mean value MRD = 0.20 %.

On the other hand, we have compared our speed of sound data with those calculated using PC-SAFT EoS (Figure 11) obtaining a mean relative deviation, MRD = 18 %. The fact that the Equations of State do not adequately represent the values (and the curvature) of this property at different pressures and temperatures is reflected in the literature [35-

39] and it is probably due to a bad representation of the pressure-volume and pressure-temperature derivatives. In order to improve the prediction of the second-order properties, some authors have modified the molecular potential function [35,36] or have included these properties in the geometrical parameters calculation [37,39]. The results showed a slight improvement in the prediction of these properties but a worsening in the VLE. Only it is observed a clear improvement when the universal constants in the dispersion term of PC-SAFT EoS were modified [37,39]. However, a wider study including more complex compounds is necessary.

Surface tension is a property of great interest in industrial processes including mass transfer so several methods and correlations have been developed for their prediction. In recent years, the Density Gradient Theory [17, 22] combined with PC-SAFT EoS has been used [40-42] to obtain σ of pure compounds or mixtures. Thus the equation of state is used to describe accurately the homogeneous system and the density gradient on the surface is determined by the functional form of the EoS and the influence parameter, $\boldsymbol{k}_{ii}$. This parameter can be obtained from theoretical considerations because it is related to the radial distribution function. However, it has been observed that calculated in this way often overestimate the value of the surface tension [43]. Therefore, it is usual to fit $\boldsymbol{k}_{ii}$ from σ experimental data. Cornelisse observed that this parameter was slightly dependent on temperature [17] Table 4 reports the dependent - temperature influence parameter of 2-acetylthiophene, $\boldsymbol{k}_{ii} = \boldsymbol{f}(\boldsymbol{T})$, calculated from our surface tension data and Figure 12 shows the comparison in the prediction. There is a good agreement between the σ experimental and calculated values with a deviation, $\boldsymbol{MRD}$ = 0.16 %. On the other hand, we have also calculated a temperature-independent influence parameter: $\boldsymbol{k}_{ii} = 3.98 \cdot 10^{-19}$ J·m^{5}·mol^{-2}. The deviation using $\boldsymbol{k}_{ii} \neq \boldsymbol{f}(\boldsymbol{T})$ was slightly higher, $\boldsymbol{MRD}$ = 0.99 % but it is also observed a clear trend with the temperature (Figure 12).

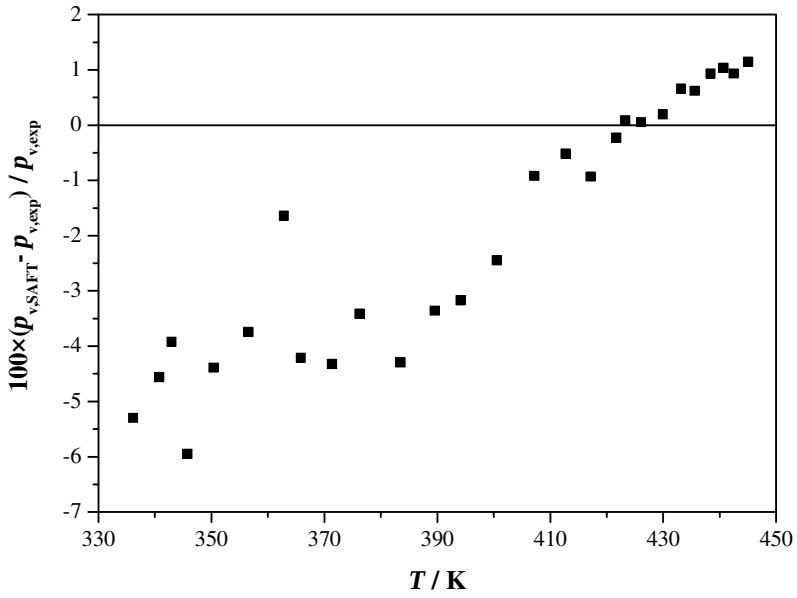

Figure 9. Deviations between experimental vapour pressures, $\boldsymbol{p}_{v,exp}$, and those calculated using PC-SAFT equation of state, $\boldsymbol{p}_{v,SAFT}$.

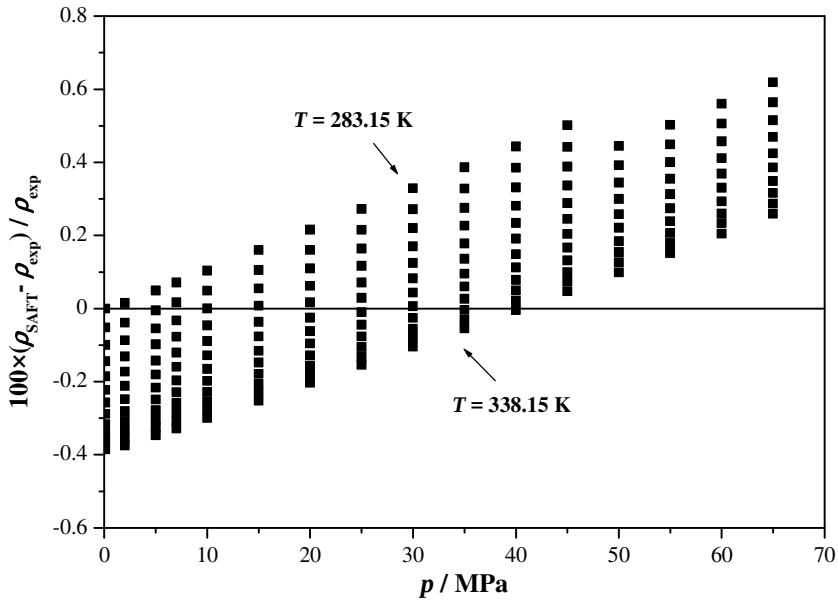

Figure 10. Deviations between experimental densities, ρ_{exp}, and those calculated using PC-SAFT equation of state, ρ_{SAFT}.

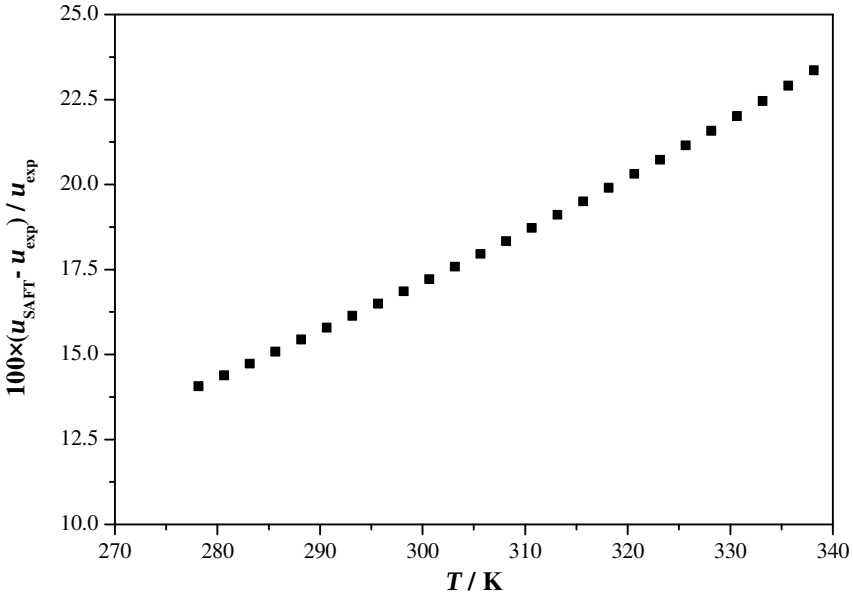

Figure 11. Deviations between experimental speeds of sound, $\boldsymbol{u}_{\mathrm{exp}}$, and those calculated using PC-SAFT equation of state, $\boldsymbol{u}_{\mathrm{SAFT}}$.

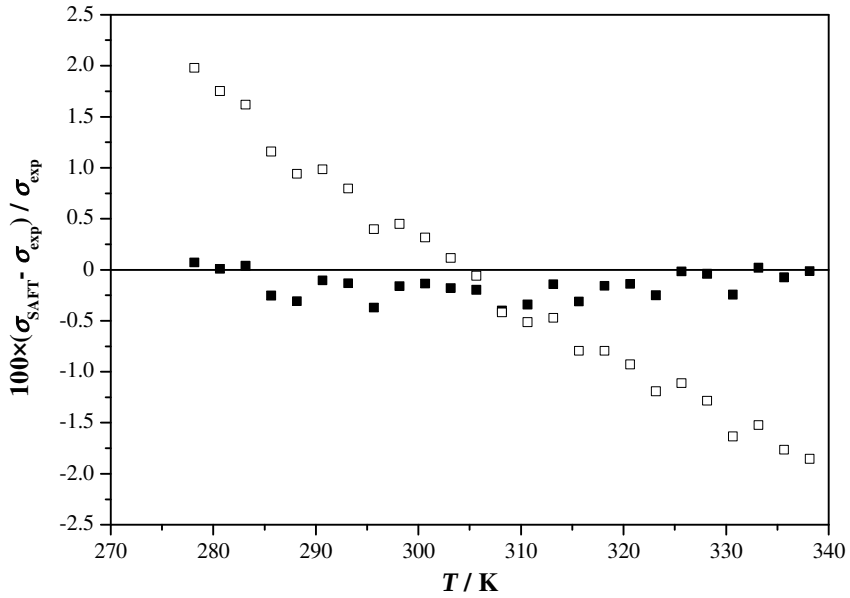

Figure 12. Deviations between experimental surface tensions, σ_{exp}, and those calculated using PC-SAFT equation of state, σ_{SAFT}.: (□) temperature-independent parameter $\boldsymbol{k}_{\mathrm{ii}}$; (■) temperature-dependent parameter $\boldsymbol{k}_{\mathrm{ii}}$.

5. Conclusions

In this study, we have reported experimental and calculated data for several thermophysical properties for 2-acetylthiophene. We have analysed the phase, volumetric and acoustic

behaviour. Also we have discussed about other properties such as the permittivity, the refractive index, the surface tension, and the absolute viscosity.

A comparison between the 2-acetylthiophene and the thiophene was carried out to understand how the introduction of the acetyl group into the ring affected at the different properties. From the results, we can conclude that the compound studied in this paper presents greater intermolecular interactions than thiophene due to interactions among the π-electrons of carbonyl group and those of aromatic ring. Consequently 2-acetylthiophene has lower vapour pressure, is more closely packed and exhibits a higher dipole moment than thiophene.

We modelled the vapour pressure, density, speed of sound and surface tension data using PC-SAFT EoS. The small values of the deviations, 0.11 kPa for the pressure, 0.24% for the density, and 0.11 % for the surface tension allowed us to conclude that this EoS adequately represents these properties in a wide range of pressures and temperatures. In contrast, the EoS provided larger deviations, 18 %, in acoustical behavior prediction.

Acknowledgements

Authors are indebted by financial support from Ministerio de Economía y Competitividad (CTQ2013-44867-P) and Gobierno de Aragón and Fondo Social Europeo "Construyendo Europa desde Aragón".

Appendix A. Supporting information

Supporting information related to this article can be found at http:// dx.doi.org/….

References

[1] T. Ohshiro, Y. Izumi, Microbial desulfurization of organic sulfur compounds in Petroleum, Biosci. Biotechnol. Biochem. 63 (1999) 1-9.

[2] M.F. Ali, A. Al-Malki, S. Ahmed, Chemical desulfurization of petroleum fractions for ultra-low sulfur fuels, Fuel. Process. Technol. 90 (2009) 536-544.

[3] W.L.P. Bredie, D.G. Mottram, R.C.E. Guy, Effect of the temperature and pH on the generation of flavor volatiles in extrusion cooking of wheat flour, J. Agric. Food. Chem. 50 (2002) 1118-1125.

[4] K. Mahadevan, L. Farmer, Key odor impact compounds in three yeast extract pastes, J. Agric. Food. Chem. 54 (2006) 7242-7250.

[5] Y. Fujima, M. Ikunaka, T. Inoue, J. Matsumoto, Synthesis of (S)-3-(N-methylamino)-1-(2-thienyl)propan-1-ol: Revisiting Eli Lilly's resolution-racemization-recycle synthesis of Duloxetine for its robust processes, Org. Process. Res. Dev. 10 (2006) 905-913.

[6] J.D. White, R. Juniku, K. Huang, J. Yang, D.T. Wong, Synthesis of 1,1-[1-Naphtyloxy-2-thiophenyl]-2-methylaminomethylcyclo-propanes and their evaluation as inhibitors of serotonin, norepinephrine, and dopamine transporters. J. Med. Chem. 52 (2009) 5872-5879.

[7] E.S. Lazer, H.Ch. Wong, G.J. Possanza, A.G. Graham, P.R. Farina, Antiinflamatory 2,6-Di-tert-butyl-4-(2-arylethenyl)phenols, J. Med. Chem. 32 (1989) 100-104.

[8] H. Hussain, A. Al-Harrasi, A. Al-Rawahi, I.R. Green, S. Gibbons, Fruitful decade for antileishmanial compounds from 2002 to late 2011, Chem. Rev. 114 (2014) 10369-10428.

[9] M.A. Esteruelas, A.M. López, M. Oliván, Polyhybrides of platinum group metals: nonclassical interactions and σ-bond activation reactions, Chem. Rev. 2016 (doi: 10.1021/acs.chemrev.6b00080).

[10] C. Allais, J.M. Grassot, J. Rodriguez, T. Constantieux, Metal-free multicomponent syntheses of pyridines, Chem. Rev. 114 (2014) 10829-10868.

[11] G.C. Johnson, Physical properties of 2-acetylthiophene, J. Amer. Chem. Soc. 69 (1947) 150-152.

[12] M.V. Roux, M. Temprado, P. Jiménez, R. Notario, J.S. Chickos, A. Filipa, L.O.M. Santos, M.A.V. Ribeiro da Silva, Thermochemistry of 2- and 3-acetylthiophenes: Calorimetric and computational study, J. Phys. Chem. A 111 (2007) 11084-11092.

[13] B. Giner, C. Lafuente, A. Villares, M. Haro, M.C. Lopez, Volumetric and refractive properties of binary mixtures containing 1,4-dioxane and chloroalkanes, J. Chem. Thermodyn. 39 (2007) 148-157.

[14] B.Giner, S. Martin, H. Artigas, M.C. Lopez, C. Lafuente, Study of weak molecular interactions through thermodynamic mixing properties, J. Phys. Chem. B 110 (2006) 17683-17690.

[15] G.Yu, D. Zhao, L. Wen, S. Yang, K. Chen, Viscosity of ionic liquids: database, observation and quantitative structure-property relationship analysis, AIChE. J. 58 (2012) 2885-2899.

[16] J. Gross, G. Sadowski, Perturbed-chain SAFT: An equation of state based on a perturbation theory for chain molecules, Ind. Eng. Chem. Res. 40 (2001) 1244-1260.

[17] P.M.W. Cornelisse, Ph. Thesis, Delft University of Technology, Delft, The Netherlands, 1997.

[18] H. Guerrero, C. Lafuente, F. Royo, L. Lomba, B. Giner, $p\rho T$ behavior of several chemical form biomass, Energy & Fuels 25 (2011) 3009-3013.

[19] W.G. Chapman, G. Jackson, K.E. Gubbins, Phase equilibria of associating fluids, Mol. Phys. 65 (1988) 1057-1079.

[20] J.A. Barker, D. Henderson, Perturbation theory and equation of state for fluids: the square-well potential, J. Chem. Phys. 47 (1967) 2856-2861.

[21] J.A. Barker, D. Henderson, Perturbation theory and equation of state for fluids. II. A successful theory of liquids, J. Chem. Phys. 47 (1967) 4714-4721.

[22] J.W Cahn, J.E Hilliard, Free energy of a nonuniform system. I. Interfacial free energy, J. Chem. Phys., 28 (1958), 258–267.

[23] V. Antón, H. Artigas, L. Lomba, B. Giner, C. Lafuente, Thermophysical properties of the thiophene family, J. Therm. Anal. Calorim. 125 (2016) 509-518.

[24] E.C. Ihmels, J. Gmehling, Densities of toluene, carbon dioxide, carbonyl sulfide, and hydrogen sulfide over a wide temperature and pressure range in the sub- and supercritical state, Ind. Eng. Chem. Res. 40 (2001) 4470-4477.

[25] J. Dymond, R. Malhotra, The Tait equation – 100 years on, Int. J. Thermophys. 9 (1988) 941–951.

[26] H.G. Rackett, Equation of state for saturated liquids, J. Chem. Eng. Data 15 (1970) 514-517.

[27] C.F. Spencer, R.P. Danner, Improved equation for prediction of saturated liquid density, J. Chem. Eng. Data 17 (1972) 236-241.

[28] L. Onsager, Electric moments of molecules in liquids, J. Am. Chem. Soc. 58 (1936) 1486-1493.

[29] L. Pauling, The Nature of the Chemical Bond and the Structure of Molecules and Crystals: an Introduction to Modern Structural Chemistry, third edition, Cornell University Press: Ithaca, New York, 1948.

[30] B. Esteban, J.R. Riba, G. Baquero, R. Puig, A. Rius, Charaterization of the surface tension of vegetable oils to be used as fuel in diesel engines, Fuel 102 (2012) 231-238.

[31] H. Vogel, Das temperaturabhängigkeitsgesetz der viskosität von flüssigkeiten, Physik. Z. 22 (1921) 645-646.

[32] G.Tammann, W. Hesse, Die abhängigkeit der viscosität von der temperatur bie unterkühlten flüssigkeiten, Z. Anorg. Allg. Chem. 156 (1926) 245-257.

[33] G.S. Fulcher, Analysis of recent measurements of the viscosity of glasses, J. Am. Ceram. Soc. 8 (1925) 339-355.

[34] J.P. Grolier, O. Kiyohara, G.C. Benson, Thermodynamic properties of binary mixtures containing ketones II. Excess enthalpies of some aromatic ketones + n-hexane, + benzene, and + tetrachloromethane, J. Chem. Thermodyn. 9 (1977) 697-703.

[35] T. Lafitte, D. Bessieres, M.M. Piñeiro, J.L. Daridon, Simultaneous estimation of phase behavior and second-derivative properties using the statistical associating fluid theory with variable range approach, J. Chem. Phys. 124 (2006) 024509.

[36] T. Lafitte, M.M. Piñeiro, J.L. Daridon, D. Bessieres, A comprehensive description of chemical association effects on second derivative properties of alcohols through a SAFT-VR approach, J. Chem. Phys. B 111 (2007) 3447-3461.

[37] X. Liang, B. Maribo-Mogensen, K. Thomsen, W. Yan, G.M. Kontogeorgis, Approach to improve speed of sound calculation within PC-SAFT framework. Ind. Eng. Chem. Res. 51 (2012) 14903-14914.

[38] X. Liang, K. Thomsen, W. Yan, G.M. Kontogeorgis, Prediction of the vapor-liquid equilibria and speed of sound in binary systems of 1-alkanols and n-alkanes with the simplified PC-SAFT equation of state, Fluid Phase Equilib. 360 (2013) 222-232.

[39] X. Liang, G.M. Kontogeorgis, New variant of the universal constants in the perturbed chain-statistical associating fluid theory equation of state, Ind. Eng. Chem. Res. 54 (2015) 1373-1384.

[40] D. Fu, Investigation of surface tensions for pure associating fluids by perturbed-chain statistical associating fluid theory combined with density-gradient theory, Ind. Eng. Chem. Res. 46 (2007) 7378-7383.

[41] D. Fu, Y. Wei, Investigation of vapor−liquid surface tension for carbon dioxide and hydrocarbon mixtures by perturbed-chain statistical associating fluid theory combined with density-gradient theory, Ind. Eng. Chem. Res. 47 (2008) 4490-4495.

[42] D. Fu, H. Jiang, B. Wang, S. Fu, Investigation of the surface tension of methane and n-alkane mixtures by perturbed-chain statistical associating fluid theory combined with density-gradient theory, Fluid Phase Equilib. 279 (2009) 136-140.

[43] B. Breure, C.J. Peters, Modeling of the surface tension of pure compounds and mixtures using the density gradient theory combined with a theoretically derived influence parameter correlation, Fluid Phase Equilib. 334 (2012) 189-196.

List of symbols

$\tilde{a}$	dimensionless Helmholtz energy
A, B, C	fitting parameters of the correlation equations
A_R	parameter of the modified Rackett equation ($kg \cdot m^{-3}$)
b_0, b_1,…	parameters of the TRIDEN equation (MPa)
B_R, C_R, D_R	parameters of the modified Rackett equation
C	parameter of the TRIDEN equation
E_T	parameter of the TRIDEN equation for reducing the temperature (K)
k	Boltzmann's constant ($\approx 1.38065 \times 10^{-23}$ $J \cdot K^{-1}$)
k_{ii}	temperature-dependent influence parameter ($J \cdot m^5 \cdot mol^{-2}$)
M	molar mass ($g \cdot mol^{-1}$)
m	number of monomers of a molecule
MRD	mean relative deviations (%)
n	number of experimental points
n_D	refractive index
p	pressure (MPa)
p_0	pressure of reference (= 0.1 MPa)
p_v	vapour pressure (kPa)
T	temperature (K)
u	speed of sound ($m \cdot s^{-1}$)

Greek letters

α_p	isobaric expansibility (kK^{-1})
ε	static permitivity

ε_{SAFT}	segment energy (J)
κ_T	isothermal compressibility (TPa^{-1})
κ_S	isentropic compressibility (TPa^{-1})
η	dynamic viscosity (mPa·s)
ν	kinematic viscosity ($mm^2 \cdot s^{-1}$)
μ	dipole moment (D)
ρ	density ($kg \cdot m^{-3}$)
ρ_0	reference density ($kg \cdot m^{-3}$)
σ	surface tension ($mN \cdot m^{-1}$)
σ_{SAFT}	segment diameter (Å)

Subscripts

cal	calculated
exp	experimental
lit	literature
SAFT	statistical associated fluid theory

Superscripts

assoc	association contribution
dis	dispersive attractive contribution
hc	hard-chain contribution
id	ideal contribution
polar	polar contribution
res	residual contribution

Thermophysical study of

2-acetylthiophene: experimental and modelled results

V. Antón, H. Artigas, J. Muñoz-Embid, M. Artal, C. Lafuente*

Departamento de Química Física, Facultad de Ciencias, Universidad de Zaragoza, 50009 Zaragoza, Spain.

*Corresponding author. Tel: +34 976762295, E-mail address: celadi@unizar.es

Table S1. Experimental vapour pressure of 2-acetylthiophene as a function of temperature

T / K	p_v / kPa	T / K	p_v / kPa	T / K	p_v / kPa	T / K	p_v / kPa
336.16	0.305	365.84	1.545	407.19	9.015	433.16	22.200
340.77	0.400	371.37	2.020	412.74	11.050	435.59	24.035
342.94	0.450	376.26	2.520	417.12	13.015	438.37	26.190
345.74	0.540	383.49	3.530	421.69	15.195	440.66	28.125
350.41	0.690	389.55	4.545	423.25	15.990	442.49	29.805
356.58	0.955	394.16	5.500	426.08	17.630	445.02	32.160
362.84	1.295	400.53	7.065	429.93	20.045		

[a]Standard uncertainties u are $u(T) = 0.01$ K, $u(p) = 0.05$ kPa

Table S2. Experimental and derived thermophysical properties of 2-acetylthiophene at $\boldsymbol{p}$ = 0.1 MPa as a function of temperature

$\boldsymbol{T}$ / K	ρ / (kg·m^{-3})	$\boldsymbol{u}$ / (m·s^{-1})	κ_S / TPa^{-1}	$\boldsymbol{n_D}$	σ / (mN·m^{-1})	$\Delta \boldsymbol{H}_\sigma$ / (mN·m^{-1})	ε	μ / D	$\boldsymbol{v}$ / (mm^2· s^{-1})	η / (mPa·s)
278.15	1185.43	1538.32	356.48		45.41	77.23	32.38		3.7170	4.3885
280.65	1183.04	1529.71	361.23		45.14	77.25	32.01		3.4554	4.0713
283.15	1180.64	1521.22	366.01	1.5705	44.83	77.23	31.64	3.89	3.2191	3.7852
285.65	1178.25	1512.70	370.90	1.5692	44.58	77.26	31.28	3.89	3.0122	3.5347
288.15	1175.86	1503.86	376.04	1.5680	44.31	77.28	30.87	3.88	2.8194	3.3017
290.65	1173.47	1495.02	381.27	1.5670	44.01	77.26	30.47	3.88	2.6484	3.0952
293.15	1171.07	1486.29	386.55	1.5658	43.73	77.27	29.94	3.87	2.5246	2.9444
295.65	1168.68	1477.76	391.83	1.5646	43.46	77.29	29.69	3.87	2.3558	2.7419
298.15	1166.29	1469.02	397.32	1.5633	43.16	77.27	29.19	3.87	2.2285	2.5884
300.65	1163.91	1460.48	402.80	1.5622	42.86	77.26	28.92	3.87	2.1081	2.4436
303.15	1161.52	1451.85	408.44	1.5609	42.59	77.27	28.47	3.86	2.0019	2.3157
305.65	1159.13	1443.23	414.19	1.5599	42.31	77.28	28.14	3.86	1.9049	2.1989
308.15	1156.74	1434.75	419.96	1.5586	42.03	77.29	27.76	3.86	1.8146	2.0903
310.65	1154.35	1426.11	425.95	1.5573	41.72	77.26	27.43	3.86	1.7310	1.9899
313.15	1151.96	1417.54	432.01	1.5562	41.43	77.26	27.05	3.85	1.6554	1.8990
315.65	1149.57	1408.95	438.20	1.5550	41.14	77.25	26.75	3.85	1.5844	1.8138
318.15	1147.18	1400.28	444.57	1.5538	40.87	77.27	26.32	3.84	1.5182	1.7344

320.65	1144.79	1391.80	450.94	1.5526	40.58	77.27	25.95	3.83	1.4572	1.6612
323.15	1142.39	1383.36	457.42	1.5514	40.27	77.24	25.68	3.83	1.4000	1.5927
325.65	1140.00	1374.95	464.00	1.5502	39.97	77.23	25.33	3.83	1.3468	1.5289
328.15	1137.61	1366.54	470.72	1.5490	39.7	77.24	25.02	3.83	1.2970	1.4692
330.65	1135.21	1358.12	477.58	1.5480	39.43	77.26	24.70	3.82	1.2499	1.4129
333.15	1132.81	1349.53	484.71	1.5468	39.12	77.24	24.33	3.81	1.2060	1.3604
335.65	1130.41	1340.79	492.09	1.5455	38.88	77.28	23.98	3.81	3.7170	1.3113
338.15	1128.01	1332.21	499.51	1.5443	38.58	77.27	23.60	3.79	3.4554	1.2647

[a]Standard uncertainties $\boldsymbol{u}$ are $\boldsymbol{u}(\boldsymbol{T})$ = 0.005 K for density and speed of sound and $\boldsymbol{u}(\boldsymbol{T})$ = 0.01 K for the rest of properties, $\boldsymbol{u}(\boldsymbol{p})$ = 0.5 kPa, and the combined expanded uncertainties $\boldsymbol{U}_c$ are $\boldsymbol{U}_c(\rho)$= 0.1 kg·m^{-3}, $\boldsymbol{U}_c(\boldsymbol{u})$ = 0.5 m·s^{-1}, $\boldsymbol{U}_c(\boldsymbol{n}_D)$ = 10^{-4}, $\boldsymbol{U}_c(\sigma)$ = 1%, $\boldsymbol{U}_c(\varepsilon)$ = 1 %, $\boldsymbol{U}_c(\nu)$ = 1%, $\boldsymbol{U}_c(\eta)$ = 1% with 0.95 level of confidence (k=2).

Table S3. Experimental densities, ρ, of 2-acetylthiophene as a function of temperature, T, and pressure, p

T / K	ρ / g·cm^{-3} at p / MPa															
	0.1	2.0	5.0	7.0	10.0	15.0	20.0	25.0	30.0	35.0	40.0	45.0	50.0	55.0	60.0	65.0
283.15	1180.61	1181.78	1183.44	1184.54	1186.17	1188.81	1191.40	1193.92	1196.37	1198.77	1201.11	1203.39				
288.15	1175.97	1177.04	1178.73	1179.85	1181.52	1184.21	1186.85	1189.43	1191.93	1194.37	1196.76	1199.09				
293.15	1171.00	1172.28	1174.02	1175.16	1176.85	1179.61	1182.30	1184.93	1187.48	1189.98	1192.41	1194.78	1197.10	1199.35	1201.56	1203.71
298.15	1166.24	1167.52	1169.28	1170.46	1172.20	1175.02	1177.77	1180.44	1183.06	1185.59	1188.08	1190.50	1192.87	1195.17	1197.42	1199.61
303.15	1161.59	1162.77	1164.60	1165.79	1167.56	1170.45	1173.26	1175.98	1178.65	1181.25	1183.77	1186.24	1188.64	1190.99	1193.27	1195.50
308.15	1156.84	1158.03	1159.89	1161.11	1162.92	1165.87	1168.75	1171.53	1174.24	1176.89	1179.46	1181.98	1184.43	1186.82	1189.15	1191.41
313.15	1152.05	1153.30	1155.19	1156.45	1158.29	1161.33	1164.23	1167.08	1169.85	1172.56	1175.19	1177.74	1180.24	1182.67	1185.04	1187.36
318.15	1147.15	1148.56	1150.49	1151.77	1153.65	1156.74	1159.72	1162.64	1165.47	1168.21	1170.90	1173.50	1176.04	1178.53	1180.93	1183.29
323.15	1142.34	1143.79	1145.78	1147.09	1149.02	1152.17	1155.23	1158.22	1161.08	1163.89	1166.63	1169.28	1171.88	1174.40	1176.86	1179.25
328.15	1137.56	1139.02	1141.06	1142.39	1144.38	1147.60	1150.78	1153.79	1156.77	1159.56	1162.34	1165.07	1167.69	1170.28	1172.79	1175.21
333.15	1132.76	1134.24	1136.33	1137.70	1139.72	1143.11	1146.25	1149.39	1152.35	1155.23	1158.08	1160.83	1163.52	1166.14	1168.68	1171.17
338.15	1127.97	1129.47	1131.61	1133.01	1135.08	1138.55	1141.78	1144.86	1147.94	1150.94	1153.82	1156.64	1159.38	1162.04	1164.64	1167.11

[a] Standard uncertainties u are $u(T)$ = 0.01 K, $u(p)$ = 0.05 MPa, and the combined expanded uncertainties U_c are $U_c(\rho)$ = 0.2 kg· m^{-3}, with 0.95 level of confidence (k=2).

Table S4. Calculated isobaric expansibilities, α_p, of 2-acetylthiophene as a function of temperature, ***T***, and pressure, ***p***

T / K	α_p / kK^{-1} at ***p*** / MPa															
	0.1	2.0	5.0	7.0	10.0	15.0	20.0	25.0	30.0	35.0	40.0	45.0	50.0	55.0	60.0	65.0
283.15	0.8096	0.8043	0.7963	0.7911	0.7836	0.7718	0.7606	0.7502	0.7404	0.7311	0.7223	0.7140				
288.15	0.8129	0.8074	0.7991	0.7937	0.7860	0.7737	0.7623	0.7515	0.7414	0.7319	0.7230	0.7145				
293.15	0.8162	0.8106	0.8020	0.7964	0.7884	0.7758	0.7640	0.7530	0.7426	0.7329	0.7237	0.7150	0.7068	0.6990	0.6917	0.6846
298.15	0.8197	0.8138	0.8049	0.7992	0.7909	0.7779	0.7658	0.7545	0.7439	0.7339	0.7246	0.7157	0.7074	0.6994	0.6919	0.6848
303.15	0.8231	0.8171	0.8079	0.8020	0.7935	0.7802	0.7678	0.7562	0.7453	0.7351	0.7256	0.7166	0.7081	0.7000	0.6924	0.6852
308.15	0.8267	0.8205	0.8110	0.8050	0.7962	0.7825	0.7698	0.7580	0.7469	0.7365	0.7268	0.7176	0.7090	0.7008	0.6931	0.6858
313.15	0.8303	0.8239	0.8142	0.8080	0.7990	0.7850	0.7720	0.7599	0.7486	0.7381	0.7282	0.7189	0.7102	0.7019	0.6941	0.6867
318.15	0.8341	0.8275	0.8175	0.8111	0.8020	0.7876	0.7744	0.7621	0.7506	0.7399	0.7299	0.7205	0.7117	0.7033	0.6955	0.6880
323.15	0.8379	0.8311	0.8209	0.8144	0.8051	0.7905	0.7770	0.7645	0.7528	0.7420	0.7319	0.7224	0.7135	0.7051	0.6972	0.6897
328.15	0.8418	0.8349	0.8245	0.8178	0.8083	0.7935	0.7798	0.7671	0.7554	0.7444	0.7342	0.7247	0.7157	0.7073	0.6994	0.6919
333.15	0.8458	0.8388	0.8282	0.8214	0.8117	0.7967	0.7829	0.7701	0.7582	0.7473	0.7370	0.7274	0.7184	0.7100	0.7021	0.6946
338.15	0.8499	0.8428	0.8320	0.8252	0.8154	0.8002	0.7862	0.7734	0.7615	0.7505	0.7402	0.7307	0.7217	0.7133	0.7054	0.6979

Table S5. Calculated isothermal compressibilities, κ_T, of 2-acetylthiophene as a function of temperature, T, and pressure, p

T / K	κ_T / TPa^{-1} at p / MPa															
	0.1	2.0	5.0	7.0	10.0	15.0	20.0	25.0	30.0	35.0	40.0	45.0	50.0	55.0	60.0	65.0
283.15	491.03	484.36	474.19	467.66	458.20	443.28	429.34	416.28	404.01	392.47	381.60	371.33				
288.15	505.37	498.30	487.55	480.65	470.66	454.94	440.27	426.55	413.68	401.60	390.22	379.50				
293.15	520.23	512.74	501.36	494.07	483.52	466.95	451.51	437.10	423.60	410.95	399.05	387.84	377.27	367.28	357.82	348.86
298.15	535.61	527.67	515.63	507.92	496.78	479.31	463.06	447.92	433.76	420.51	408.06	396.36	385.33	374.92	365.08	355.76
303.15	551.51	543.10	530.36	522.20	510.44	492.01	474.91	459.00	444.15	430.27	417.26	405.03	393.53	382.69	372.44	362.75
308.15	567.92	559.01	545.52	536.89	524.47	505.04	487.04	470.33	454.76	440.22	426.61	413.85	401.86	390.56	379.91	369.84
313.15	584.84	575.39	561.11	551.99	538.87	518.38	499.44	481.89	465.56	450.34	436.12	422.80	410.30	398.54	387.46	377.00
318.15	602.24	592.23	577.11	567.47	553.61	532.01	512.09	493.66	476.55	460.62	445.76	431.86	418.84	406.60	395.08	384.21
323.15	620.10	609.50	593.50	583.30	568.68	545.91	524.96	505.61	487.69	471.03	455.51	441.02	427.45	414.71	402.75	391.47
328.15	638.39	627.16	610.23	599.46	584.02	560.05	538.03	517.73	498.96	481.54	465.34	450.23	436.11	422.87	410.45	398.75
333.15	657.07	645.17	627.27	615.90	599.62	574.38	551.25	529.97	510.32	492.13	475.23	459.49	444.80	431.05	418.15	406.03
338.15	676.07	663.49	644.57	632.57	615.41	588.86	564.58	542.28	521.74	502.75	485.14	468.76	453.49	439.21	425.84	413.28